International Journal of
Molecular Sciences

MDPI

Article

Unravelling the Role of Habenula Subnuclei on Avoidance Response: Focus on Activation and Neuroinflammation

Geiza Fernanda Antunes [1,†], Ana Carolina Pinheiro Campos [1,†], Daniel de Oliveira Martins [1], Flavia Venetucci Gouveia [1,2], Miguel José Rangel Junior [3,4], Rosana Lima Pagano [1] and Raquel Chacon Ruiz Martinez [1,5,*]

1 Division of Neuroscience, Hospital Sírio-Libanês, Sao Paulo 01308-060, Brazil
2 Neurosciences and Mental Health, The Hospital for Sick Children, Toronto, ON M5G 0A4, Canada
3 Centro Universitário de Santa Fé do Sul, Santa Fé do Sul 15775-000, Brazil
4 Medical School, Universidade Brasil, Fernandópolis 15600-000, Brazil
5 Laboratorios de Investigação Médica—LIM/23, Institute of Psychiatry, School of Medicine, University of Sao Paulo, Sao Paulo 05508-900, Brazil
* Correspondence: quelmartinez@yahoo.com.br
† These authors contributed equally to this work.

Abstract: Understanding the mechanisms responsible for anxiety disorders is a major challenge. Avoidance behavior is an essential feature of anxiety disorders. The two-way avoidance test is a preclinical model with two distinct subpopulations—the good and poor performers—based on the number of avoidance responses presented during testing. It is believed that the habenula subnuclei could be important for the elaboration of avoidance response with a distinct pattern of activation and neuroinflammation. The present study aimed to shed light on the habenula subnuclei signature in avoidance behavior, evaluating the pattern of neuronal activation using FOS expression and astrocyte density using GFAP immunoreactivity, and comparing control, good and poor performers. Our results showed that good performers had a decrease in FOS immunoreactivity (IR) in the superior part of the medial division of habenula (MHbS) and an increase in the marginal part of the lateral subdivision of lateral habenula (LHbLMg). Poor performers showed an increase in FOS in the basal part of the lateral subdivision of lateral habenula (LHbLB). Considering the astroglial immunoreactivity, the poor performers showed an increase in GFAP-IR in the inferior portion of the medial complex (MHbl), while the good performers showed a decrease in the oval part of the lateral part of the lateral complex (LHbLO) in comparison with the other groups. Taken together, our data suggest that specific subdivisions of the MHb and LHb have different activation patterns and astroglial immunoreactivity in good and poor performers. This study could contribute to understanding the neurobiological mechanisms responsible for anxiety disorders.

Keywords: avoidance behavior; lateral habenula; medial habenula; astrocytes; neuroinflammation; neuronal activation

Citation: Antunes, G.F.; Campos, A.C.P.; Martins, D.d.O.; Gouveia, F.V.; Rangel Junior, M.J.; Pagano, R.L.; Martinez, R.C.R. Unravelling the Role of Habenula Subnuclei on Avoidance Response: Focus on Activation and Neuroinflammation. *Int. J. Mol. Sci.* **2023**, *24*, 10693. https://doi.org/10.3390/ijms241310693

Academic Editors: Yanxue Xue and Jianfeng Liu

Received: 4 April 2023
Revised: 16 May 2023
Accepted: 22 May 2023
Published: 27 June 2023

1. Introduction

Anxiety disorders are the most prevalent mental disorder, with different and complex conditions that significantly reduce the quality of life of affected individuals [1,2]. Due to its complex, heterogeneous and individualized nature, understanding the biological mechanisms that are altered in anxiety disorders is a major challenge. Avoidance behavior is an essential feature of anxiety disorders [3,4]. In preclinical research, avoidance response can be evaluated using the two-way active avoidance test [5,6]. Based on the number of avoidance responses, it is possible to differentiate two populations of animals: the good performers and the poor performers. While poor performers freeze excessively and exhibit less than 20 avoidance responses in a trial, good responders are able to learn the task and avoid the aversive stimulus [6].

It has been proposed that this behavioral distinction could be based on differential recruitment of brain circuits [7,8]. One structure that is implicated in the neuronal network of psychiatric disorders [9] and has not been well-evaluated in this paradigm is the habenula. The habenula is a limbic structure classically involved in motivation, emotion, reinforcement, learning, pain and depression [10,11]. However, it has been emerging as responsible for processing aversive stimuli in an experience-dependent selection of behavioral responses to stressors [12,13]. Based on the pattern of afferent and efferent connectivity, the habenula can be divided into several subnuclei that have distinct cellular and molecular characteristics [14–16]. These anatomical and molecular divisions highlight the complexity of the habenula [14,17], emphasizing the importance of a detailed evaluation of this structure. The habenula plays a central role in the connections between the forebrain to midbrain regions for the integration of emotional and sensory processing [18]. It is also considered a major regulatory site for serotonergic and dopaminergic neurotransmission [19,20], both of which are highly implicated in the neurobiology of anxiety disorders and avoidance behavior [21]. In line with this, it has been shown that lesions targeting the LHb facilitate avoidance responses [22], while stimulation impairs this response [23]. However, the effect of aversive learning performance in the different subnuclei of habenula remains unclear.

Another important factor that may influence habenular function is the functional integrity of astrocytes, which play an important role in immune responses, synaptic pruning and neuroplasticity [24]. It has been proposed that chronic stress induces an increased inflammatory response in the habenula [25], suggesting that glial cells could contribute to the local inflammatory profile, resulting in a maladaptive and chronic inflammatory state [26], playing an important role in chronic neuroplasticity [27].

Therefore, this study aimed to perform a broad evaluation of the neuronal activation patterns (FOS expression) and astrocyte density (GFAP immunoreactivity) in several habenula subnuclei in rats presenting good and poor performance and control animals in an aversive learning paradigm to investigate if these patterns could help explain the behavioral difference observed in these groups. Specifically, this study aimed to shed light on the habenula subnuclei signature in avoidance behavior, evaluating the pattern of neuronal activation using FOS expression and astrocyte density using GFAP immunoreactivity, and comparing control, good and poor performers.

2. Results

2.1. Behavioral Testing: Two-Way Active Avoidance Test

Based on the number of avoidance responses presented during training, animals were divided into good and poor performance groups. The good performers showed an increase in the number of avoidance responses (Group $F_{(1,17)} = 66.97$, $p < 0.001$; Session: $F_{(7,17)} = 5.97$, $p < 0.001$; Group $\times$ Session $F_{(7,17)} = 6.578$; $p = 0.0007$; Figure 1A) and a decrease in the percentage of freezing (Group: $F_{(2,32)} = 68.82$, $p < 0.001$; Session: $F_{(3,32)} = 5.36$, $p = 0.002$; Group $\times$ Session $F_{(2,32)} = 77.96$; $p < 0.0001$; Figure 1B) along the sessions.

2.2. Immunoreactivity in the Medial Habenular Complex: MHbS, MHbI, MHbC and MHbL

The medial habenular complex was evaluated in its subnuclei: MHbS, MHbI, MHbC and MHbL.

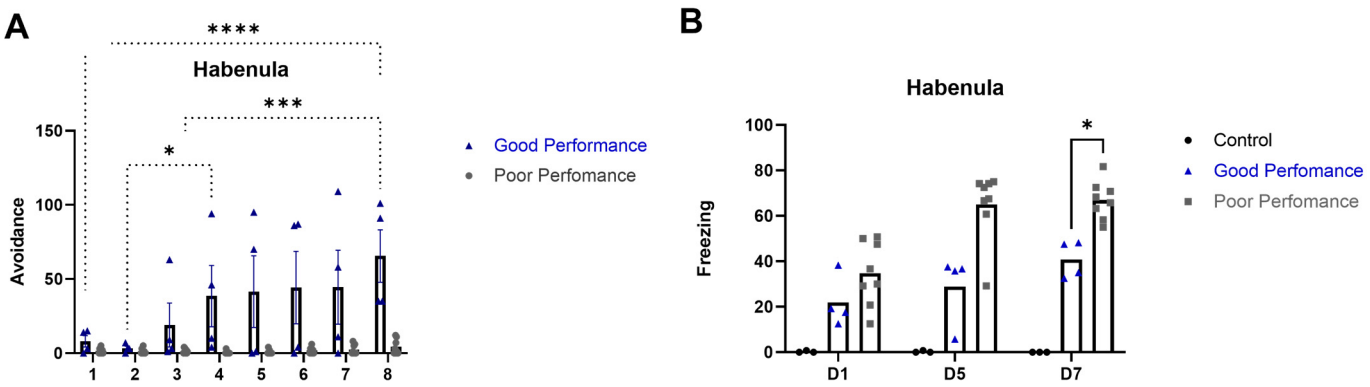

Figure 1. (**A**). Number of avoidance responses exhibited by good and poor performers animals throughout the training sessions. *, $p < 0.05$ good vs. poor performers; *** $p < 0.001$ good vs. poor performers; **** $p < 0.0001$ good vs. poor performers. (**B**). Percentage of time spent freezing in sessions 1, 5 and 7 considering control, poor and good performers. Data are presented as the mean ± standard error of the mean (SEM). *, $p < 0.001$ vs. good performance and control animals considering freezing behavior. Good performance ($n = 8$), poor performance ($n = 4$) and control ($n = 3$) animals.

2.2.1. Activation Pattern

Animals in the good performance group presented less FOS-IR in the MHbS ($F_{(2,6)} = 22.58$; $p = 0.0016$—Figure 2A) when compared with control and poor performance groups. The poor performance group showed increased FOS-IR in the MHbL ($F_{(2,8)} = 9.27$; $p = 0.0082$—Figure 2B) when compared with the control group. There was no statistical difference in FOS-IR in the MHbC ($F_{(2,8)} = 1.30$; $p = 0.32$) and MHbI ($F_{(2,8)} = 2.56$; $p = 0.14$) parts.

2.2.2. GFAP—Astroglial Immunoreactivity Pattern

Poor performance animals exhibited an increase in GFAP-IR in the MHbI ($F_{(2,7)} = 14.50$; $p = 0.0032$—Figure 2C) when compared with control and good performers. There was no statistical difference in the other regions of the MHb, MHbS ($F_{(2,9)} = 1.56$; $p = 0.26$), MHbC ($F_{(2,9)} = 1.79$; $p = 0.23$) and MHbL ($F_{(2,10)} = 0.03$; $p = 0.96$).

2.3. Immunoreactivity in the Medial Division of the Lateral Habenula: LHbMS, LHbMPc and LHbMC

The medial division of the lateral habenular complex includes the LHbMS, LHbMPc and LHbMC.

2.3.1. Activation Pattern

In LHbMS, there was an increase in FOS-IR in good performers in comparison with the control group ($F_{(2,8)} = 10.87$; $p = 0.0052$—Figure 3A). In LHbMPc, the good and poor performers showed an increased FOS-IR in comparison with control animals ($F_{(2,8)} = 20.79$; $p = 0.0007$—Figure 3B). In LHbMc, there was no difference between the groups ($F_{(2,8)} = 1.29$; $p = 0.32$).

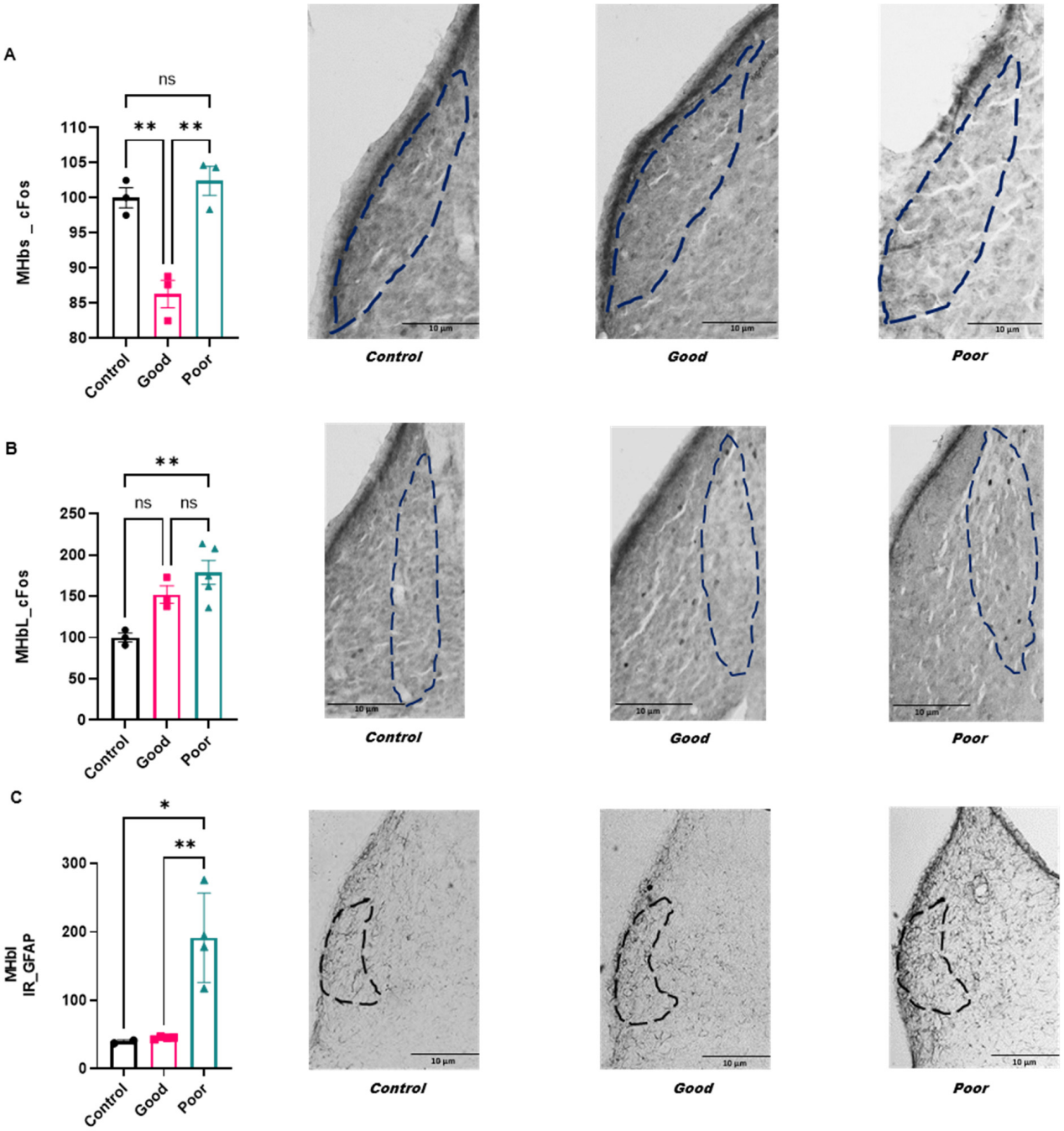

Figure 2. (**A**). FOS-IR in MHbS comparing control (n = 3), good (n = 3) and poor performance animals (n = 3). Data are presented as the mean ± standard error of the mean (SEM). (**B**). FOS-IR in MHbL of control (n = 3), good (n = 3) and poor performance animals (n = 5). (**C**). Quantification of GFAP-IR in MHbI comparing control (n = 3), good (n = 4) and poor performance animals (n = 4). The value corresponding to each animal was average, considering the right and left sides. The results were normalized by defining the control group as 100%. Data are presented as the mean ± standard error of the mean (SEM). *, $p < 0.01$; **, $p < 0.01$. Dotted lines of different colors correspond to individual animals.

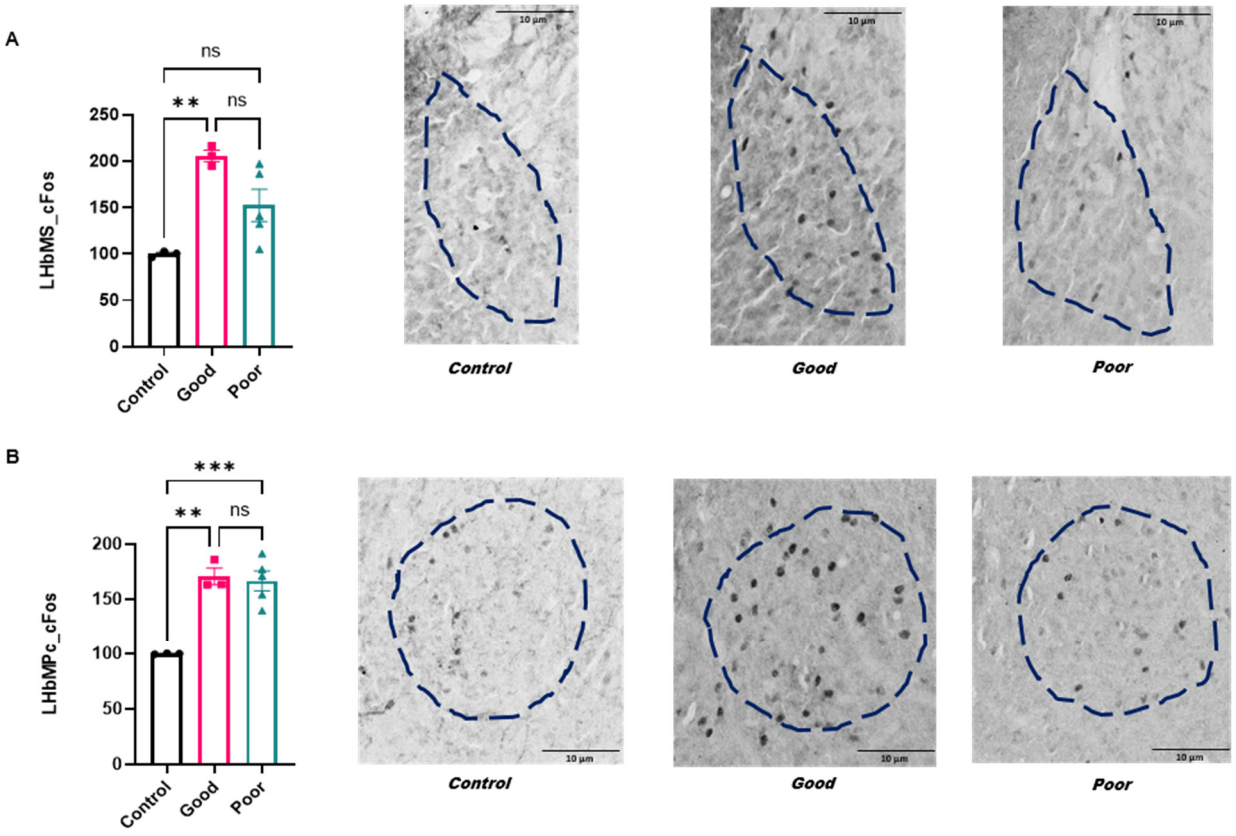

Figure 3. (**A**). FOS-IR in LHbMs. (**B**). FOS-IR in LHbMPc of control (*n* = 3), good (*n* = 3) and poor performance animals (*n* = 5). The value corresponding to each animal considers the right and left sides. The results were normalized by defining the control group as 100%. Data are presented as the mean ± standard error of the mean (SEM). ** $p < 0.01$ vs. control group; ***, $p < 0.001$ vs. poor performers. Dotted lines of different colors correspond to individual animals.

2.3.2. GFAP—Astroglial Immunoreactivity Pattern

There was no statistical difference in the IR-GFAP staining in LHbMS ($F_{(2,7)} = 2.07$; $p = 0.20$), LHbMPc ($F_{(2,8)} = 1.39$; $p = 0.30$) and LHbMC ($F_{(2,6)} = 0.90$; $p = 0.45$) between groups.

2.4. Immunoreactivity to FOS in the lateral division of the lateral habenula: LHbLMc, LHbLO, LHbLB, LHbLPc and LHbLMg

The lateral division of the lateral habenular complex includes the LHbLMc, LHbLO, LHbLB, LHbLPc and LHbLMg.

2.4.1. Activation Pattern

In the LHbLB and LHbLPc, there was an increase in FOS-IR in poor performers compared with all other groups ($F_{(2,8)} = 25.20$; $p = 0.0004$—Figure 4A; ($F_{(2,8)} = 5.19$; $p = 0.034$—Figure 4B). In the LHbLMg, the good performers showed an increase in FOS-IR in comparison with poor performers and control animals ($F_{(2,8)} = 25.20$; $p = 0.0004$—Figure 4C). No statistical difference was observed in the LHbLMc ($F_{(2,7)} = 0.026$; $p = 0.97$) and LHbLO ($F_{(2,7)} = 5.03$; $p = 0.44$).

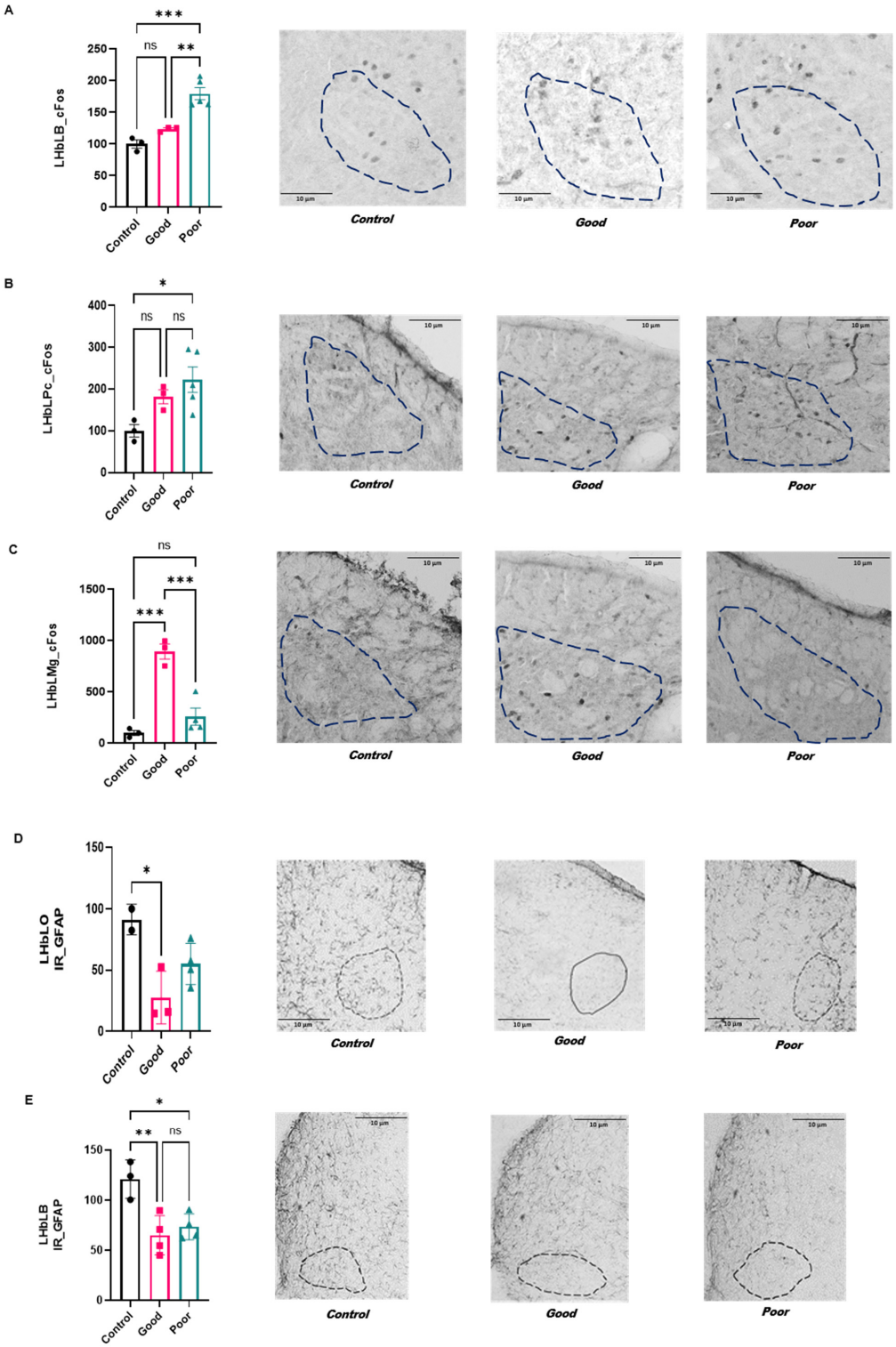

Figure 4. (**A**). FOS-IR in LHbLB, (**B**). in LHbLPc, (**C**). in LHbLMg of control (n = 3), good (n = 3) and poor performance animals (n = 4). (**D**). Quantification of GFAP-IR in LHbLB, (**E**). in LHbLO compared with control (n = 3), good (n = 4) and poor performance animals (n = 4). The value corresponding to each animal was average, considering the right and left sides. The results were normalized by defining the control group as 100%. Data are presented as the mean ± standard error of the mean (SEM). ** $p < 0.01$ vs. control group; *, $p < 0.05$; **, $p < 0.01$; ***, $p < 0.001$. Dotted lines of different colors correspond to individual animals.

2.4.2. Astroglial Immunoreactivity

The LHbLO subnuclei presented a decrease in the quantification of GFAP-IR in good performers when compared with the control group ($F_{(2,6)} = 7.570$; $p = 0.022$—Figure 4D). The LHbLB showed a reduction in IR-GFAP in good and poor performers when compared with the control group ($F_{(2,8)} = 10.07$; $p = 0.0065$—Figure 4E).

There was no statistical difference between groups in the LHbLMc ($F_{(2,7)} = 2.77$; $p = 0.13$), LHbLPc ($F_{(2,10)} = 1.36$; $p = 0.30$) and LHbLMg ($F_{(2,7)} = 4.51$; $p = 0.055$).

Table 1 summarizes the changes in behavior response, FOS-IR and GFAP-IR in good and poor performers.

Table 1. Summary data showing behavioral, FOS -IR and GFAP-IR in good and poor performers.

	Good Performers	**Poor Performers**
Behavioral Data	Increased avoidance response Decreased freezing behavior	Decreased avoidance response Increased freezing behavior
FOS-IR	Increased LHbLB Decreased MHbS	Increased LHbLB
GFAP-IR		Increased MHbI

3. Discussion

To our knowledge, our study is the first to investigate the role of habenula subnuclei in the behavioral distinction between good and poor performers in the two-way active avoidance test. Good performers displayed an increased number of avoidance responses and a decrease in the freezing response, whereas poor avoiders showed an opposite pattern [7]. Our data showed that the good performers had a decrease in FOS-IR in the MHbS and an increase in the LHbLMg, while the poor performers showed an increase in FOS-IR in the LHbLB and an increase in GFAP-IR in the MHBI. This work showed that good and poor performers have a distinct pattern of neuronal activation and astroglial reactivity in several subnuclei of the habenula.

The habenula has been shown to be involved in the modulation of avoidance behavior. Initial studies have explored lesions targeted to the habenular complex [28,29], showing impairment in avoidance response, suggesting that its connection with the limbic system is a crucial interface to evaluate the aversive stimulus [30]. Evidence over the years indicates that habenula shares more heterogeneous subdivisions and connections [31,32], highlighting the complexity and importance of the hub of connections that the habenula participates in.

3.1. The MHb Activation Pattern and Astroglial Reactivity in Good and Poor Performers in the Two-Way Aversive Learning Paradigm

Without a doubt, the role of MHb in avoidance behavior has been less investigated when compared with LHb. However, it has been shown that lesions in the MHb increased freezing behavior in zebrafish [33]. The MHb is the major habenular connection to the interpeduncular nucleus (IPN) by cholinergic and glutamatergic fibers [34,35]. Moreover, the MHb also projects into the epithalamus and LHb [17]. The IPN is an important structure of the brain that connects the habenular complex and the monoaminergic systems, contributing to the regulation of learning, sleep, reward, executive planning and fear response [14,16,36–38]. Furthermore, when considering fear and anxiety, the connection between the MHb and the posterior septum also points to the importance of the MHb in the modulation of these behaviors [33]. In this sense, Klemm [39] suggested that the interaction between the posterior septum, MHb and IPN directly reflects emotional processing and mental disorders that could occur upon failure in this pathway [39]. To better comprehend the effect of aversive learning performance in the MHb, here, we performed a subdivision of the MHb as proposed by Andres and colleagues [31]. We showed that the good performers have a decreased neuronal activation pattern in the MHbS when compared with all

the other groups. Interestingly, this is the only division of the MHb that substance P and cholinergic neurons are absent, while noradrenergic fibers and a high expression of IL-18 and GABAergic interneurons can be found [40]. However, the role of noradrenaline as a possible inhibitor on the MHb of good performers has yet to be investigated.

Interestingly, considering that our animals were evaluated after the last session (eighth session) in the shuttle-box, the decreased neuronal activation observed in these nuclei may be related to the lack of activation when the task was already learned, due to the fact that good performers had showed an increase in avoidance since the fourth session. Moreover, we found that poor performers showed an increase in FOS-IR in the MHbL and astroglial immunoreactivity in the MHbI. While both of these subdivisions have substance P and cholinergic co-expressed neurons, only the MHbL shows colocalization between glutamatergic and mu-opioid-receptor, but also P-type calcium channels, neurokinin-3 receptors and the distribution of intensely stained metenkephalin-positive fibers [40–43]. These areas containing substance P, cholinergic and glutamatergic neurons project slightly exclusively to the IPN [44], suggesting that poor performance could result in the activation of the MHb-IPN glutamatergic-cholinergic pathway. The increase in FOS-IR in poor performers may reflect the increased rate of acute freezing behavior in the last session, which suggests a participation of the MHb-IPN in fear and anxiety [45,46]. Again, further studies are needed to better comprehend the extent of each MHb-IPN projection since different neurons within the MHb have very distinct roles. For example, while the activation of GABAergic receptors in the MHb-IPN pathway induces increased neurotransmitter release in the glutamatergic-cholinergic projection, it has the opposite effect in glutamatergic-substance P projections [47]. On the other hand, the increased astroglial IR showed in poor performers may reflect maladaptive neuroplasticity from consistent stress and freezing behavior due to the failure to learn the task. Increased astroglial IR is linked to increased neuroinflammation induced by stress [48]. However, astrocytes may also increase their ramifications hours after the occurrence of long-term potentiation [49], suggesting that MHbI subnuclei may be more sensitive towards maladaptive neuroplasticity of fear and anxiety consolidation. Nevertheless, our intriguing results suggest that MHb also plays a pivotal regulatory role in avoidance behavior, where each subdivision demonstrates a particular signature.

3.2. The LHb Activation Pattern and Astroglial Reactivity in Good and Poor Performers in the Two-Way Aversive Learning Paradigm

The LHb is the major portion of the habenula, with most studies focused on aversive learning. Lesions to the LHb lead to impairment in avoidance responses [22,23]. We found that good and poor performers showed an increase in the neuronal activation pattern of the LHbMPc when compared with control animals. Considering that both good and poor performers are subjected to the avoidance protocol, it is possible to hypothesize that this activation may be related to the stress response rather than learning performance. Notably, animals were evaluated after eight sessions in the shuttle box, suggesting that LHbMPc may be sensitive to stress even after consecutive sessions. Supporting our data, it has been shown that a variety of stressor could increase FOS expression in the lateral habenula, emphasizing the close interaction with the medial prefrontal cortex, lateral septum, extended amygdala, hypothalamus and dorsal raphe [50–54]. In a similar way, both groups showed a decrease in astroglial immunoreactivity in the LHbLB. Decreased astroglial IR has been related to depressive-like behavior in different areas of the brain, but especially the hippocampus [55,56]. Additionally, astroglial activation to stress in the habenula has been shown [57,58]. Because these results were found in good and poor performers, it suggests that the chronic stress-induced disruption of pathways is independent of learning performance. Indeed, it has been shown that the LHb participates in behavioral responses such as pain, anxiety, reward and stress [50,59–61]. Although the habenular complex may not be directly involved in regulating the effects of stress on the HPA axis, this structure has been associated with a variety of behaviors that are influenced by stress, including learning,

exploratory behavior and responsiveness to aversive stimuli [62,63]. Furthermore, behaviors such as exploratory activity, responsiveness to aversive stimuli and sexual behavior present circadian variations [64] that may, in turn, be related to the activation pattern of the LHb [65].

Here, we conducted a detailed evaluation of the many subdivisions of LHb. We found that poor performers showed an increased neuronal activation pattern in the LHbLB and LHbLPc. These nuclei have distinct cell types (i.e., cholinergic and parvalbumin neurons, respectively [66]), suggesting that poor performance in avoidance behavior involves a dysregulation in the habenular complex. Moreover, both structures receive inputs from the magnocellular preoptic nucleus, which has an important role in neuroendocrine responses [67]. Notably, while good and poor performers showed a decrease in astroglial IR in the LHbLB, only poor performers showed an increase in the neuronal activation pattern. FOS-IR is often attributed to an acute response, suggesting that this subnucleus is involved in learning performance. The reduction in GFAP-IR observed in both groups may be a result of chronic stress induced by the shuttle box testing.

On the other hand, good performers showed an increase in the activation pattern in the LHbLMg and LHbMs. The LHbM nuclei receive important projections from the entopeduncular nucleus, lateral hypothalamus, areas of the limbic system and the ventral striatal complex, such as the prefrontal cortex [14,68–70]. Interestingly, the LHbMS, which is more activated in good performers, contains somatostatin, which may facilitate learning and cognitive function [71].

We found that good performers have a decrease in astroglial immunoreactivity only in the LHbLO that had a very specific innervation from the entopeduncular nucleus [66], a pivotal structure of the basal ganglia. Because the habenula-entopeduncular nucleus is often related to the aversive effect after rewarding [72], is reasonable to suppose that the decrease in astroglia in this nucleus is a neuroplasticity response to a synaptic modulation that occurs during the learning process. Thus, the activation of dopamine receptors expressed in astrocytes could be able to increase (DR1) or decrease (DR2) activation [73]. Hence, considering the role of dopamine in avoidance behavior [74] and the pivotal regulatory role of habenula in the dopaminergic system, is possible that the decrease observed in astroglial immunoreactivity is an example of an adaptive response from the aversive learning paradigm that results in a good performers in the avoidance protocol.

Limitations and Future Perspectives

An important limitation of this work is that we did not aim to identify the great number of neuronal populations activated, inhibited or affected by stress or learning performance. Rather, we aimed to demonstrate that habenular complex subnuclei show different neuronal and astroglial patterns in the paradigm of learning performance. Another important limitation of our study is that only male rats were included. It is well-known that females have a distinct response to aversive paradigms, and therefore, it is of the utmost importance that future works investigate sex differences regarding aversive learning and the regarding mechanisms and pathways involved. Future investigations should aim to understand the chronic and acute effects of avoidance and freezing behavior in the MHb-IPN pathway, focusing on the glutamatergic-cholinergic pathway and the habenular noradrenergic response. It would also be interesting to further understand the maladaptive neuroplasticity induced by chronic stress in the MHbI, LHbMPc and LHbLB. More specific work attempting to identify the cellular populations and connections involved in this paradigm is necessary to better comprehend the role of the habenular complex in stress and aversive learning.

4. Materials and Methods

4.1. Experimental Design

The experimental design is illustrated in Figure 5. After habituation to the animal facility, Wistar rats were submitted to eight daily training sessions in the two-way shuttle

box and subsequently divided into good and poor performers according to the avoidance response exhibited during the sessions. The control animals were exposed to the two-way shuttle box, but the footshock was turned off. On the eighth day, 90 min after the end of the testing session, animals were anesthetized, perfused and the brains were collected for future analysis. Brains were sliced in a freezing microtome and processed for determination of histological landmarks (Nissl-stained), neuronal activation (FOS) and astrocyte density (GFAP) in order to compare control, good and poor performers. The immunoreactivity was evaluated in habenula's medial and lateral complexes.

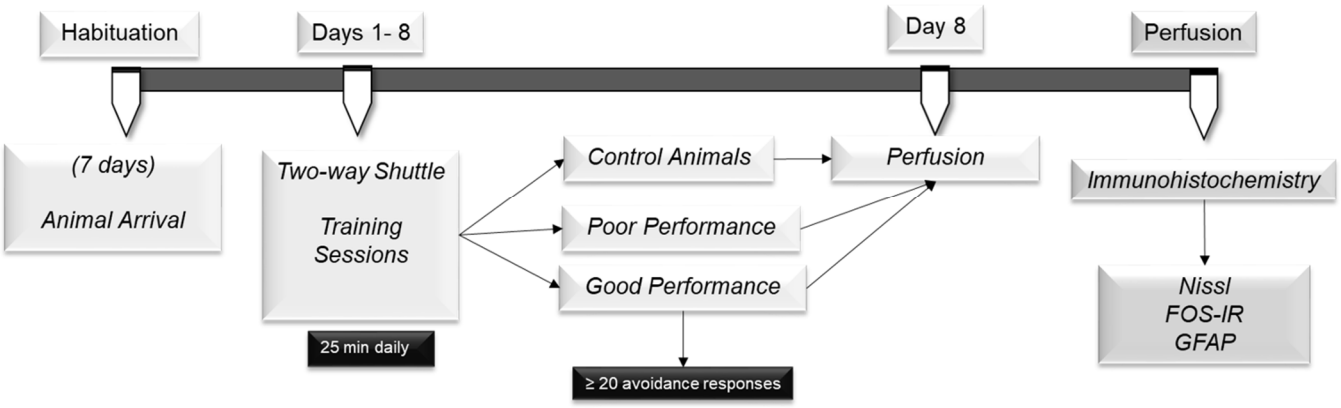

Figure 5. Experimental design of the study. After habituation to the animal facility, animals were submitted to eight daily training sessions in the two-way shuttle box. On the eighth day, 90 min after the end of the session, animals were anesthetized and perfused and the brains were processed for determination of histological landmarks (Nissl-stained), neuronal activation (FOS) and astrocyte density (GFAP).

4.2. Animals

Male Wistar rats weighing 200–300 g were housed in polypropylene cages (40 × 34 × 17 cm) in groups of three. The room temperature was maintained at 24 °C ± 1 °C under a 12:12 dark/light cycle; wood shavings and free access to food and water were provided throughout the experiment. Animals were maintained for 7 days before experiments for habituation. All animal experiments were conducted and reported in accordance with the ARRIVE guidelines (http://www.nc3rs.org.uk/arrive-guidelines), accessed on 1 March 2022. The protocols used in this project were approved by the Ethics Committee on the Use of Animals at Hospital Sirio-Libanes (CEUA #2013/12).

4.3. Two-Way Active Avoidance Test

The paradigm was performed as previously described [75]. In brief, animals were submitted to 25 min training sessions once a day for 8 consecutive days in a two-way shuttle box (Insight Equipment, Ribeirao Preto, Brazil). Shuttling between compartments delayed the delivery of scrambled footshock unconditioned stimulus (US, 0.6 mA; 0.5 s) by 30 s. In the absence of shuttling, US delivery occurred every 5 s. The response-to-stimulus interval (R–S) shuttles comprised avoidance responses, and the stimulus-to-stimulus interval (S–S) shuttles comprised escape responses. All shuttles produced 0.3 s feedback stimuli (house light blink). Controls animals were exposed to the two-way shuttle box, but the footshock was turned off (i.e., without behavior contingency). Animals performing more than 20 avoidance responses in a session for 2 consecutive days were considered good performers, while animals that did not achieve this number were considered poor performers [7,75,76]. Freezing, defined as the absence of movement except that required for breathing [77], was assessed during the first 2 min of the tests [74,76].

4.4. Perfusion

Ninety minutes after the end of the last session, all groups of animals, including control, good and poor performers, were deeply anesthetized with thiopental (40 mg/kg) and morphine sulphate (10 mg/mL) and transcardiacally perfused with a solution of 0.9% phosphate-buffered solution followed by 4.0% paraformaldehyde in 0.1 M phosphate buffer, using a peristaltic pump (Cole Parmer, Vernon Hills, IL, USA,). Brains were removed, placed in paraformaldehyde for 3 h and then transferred to a 30% sucrose/0.1 M phosphate buffer at 4 °C.

4.5. Microtomy

Frozen whole brain coronal sections (30 µm thick) were sliced with a sliding microtome (Leica SM 2000 R; Biosystems, Nussloch, Germany), collected and stored free-floating in PB 0.01 M for immunohistochemical assay.

4.6. Immunohistochemistry

Brain sections were processed overnight with anti-FOS antiserum raised in rabbit (Ab-5, Calbiochem, lot-D07099, Darmstadt, Germany; dilution 1:20,000) or mouse anti-GFAP (Sigma-Aldrich, Burlington, USA, catalogue# C9205, dilution: 1:1000) followed by incubation in appropriate biotinylated secondary antibody (Jackson ImmunoResearch, Ely, UK; dilution: 1:200) at room temperature for 2 h and avidin-biotin-peroxidase complex (ABC, Vector Laboratories, Newark, USA). The antibody complex was visualized via exposure to a chromogen solution containing 0.02% 3,3′-diaminobenzidine tetrahydrochloride (DAB; Sigma) in 0.05 M Tris-buffer (pH 7.6) and 0.01% hydrogen peroxide. Extensive washing in PBS buffer (pH 7.4) halted the DAB reaction. Additionally, a separate slide was used for negative reagent controls. The immunohistochemistry process was based on previous published guidelines of recommendations [78,79]. It includes the choice of the antibody titration to optimize the concentration and have the best measure of expression levels, using a commercially prepared and validated kit for performing the immunohistochemistry, including negative controls to identify any background staining. Additionally, the antibody cross reactivity was also evaluated using the percentage homology of the antibody immunogen to other similar proteins. We have used this same process through the years with the same care [7,11,74,80–82]. Sections were mounted on gelatin-coated slides, dehydrated and coverslipped with DPX (Sigma).

4.7. Quantification

Images were captured using a light microscope (E1000, Nikon, NY, USA) and quantification was performed using ImageJ software (News Version 1.44b National Institutes of Health, MD, USA; http://rsbweb.nih.gov/ij/, accessed on December 2022). An observed blinded-to-group allocation analyzed the FOS immunoreactivity (FOS-IR) and GFAP immunoreactivity (GFAP-IR) of the habenula subnuclei. FOS-IR was analyzed with stereology in 3–5 coronal sections per animal. GFAP-IR was analyzed using the threshold plug-in available in ImageJ software. For that, the background was subtracted from the images and the threshold was highlighted to type a known range of pixel intensities, then the particles were analyzed and the total of all particles was provided by the ImageJ. Additionally, the delineation of the habenula was performed and the corresponding area measurements were performed. The results were normalized by defining the control group as 100%. Border delineation, cell counting and area measurements were conducted with Image-J software (Version 1.44b). Adjoining Nissl-stained sections provided histological landmarks for the accurate identification and delineation of habenula subnuclei [31]. Figure 6 shows the subdivisions of the habenula. The habenula was first divided into medial (MHb) and lateral (LHb) regions. The medial complex (MHb) was divided into superior (MHbS), inferior (MHbI), central (MHbC) and lateral (MHbL) regions. The lateral complex (LHb) was subdivided into lateral (LHbL) and medial (LHbM) subdivisions and further parcellated into smaller subnuclei. The LHbL was divided into magnocellular (LHbLMc), oval (LHbLO),

basal (LHbLB), parvocellular (LHbLPc) and marginal (LHbLMg) parts. The LHbM was parcellated into superior (LHbMS), parvocellular (LHbMPc) and central (LHbMC) parts. The corresponding Bregmas were from −3.00 mm to −4.36 mm, according to the Paxinos and Watson Atlas [83].

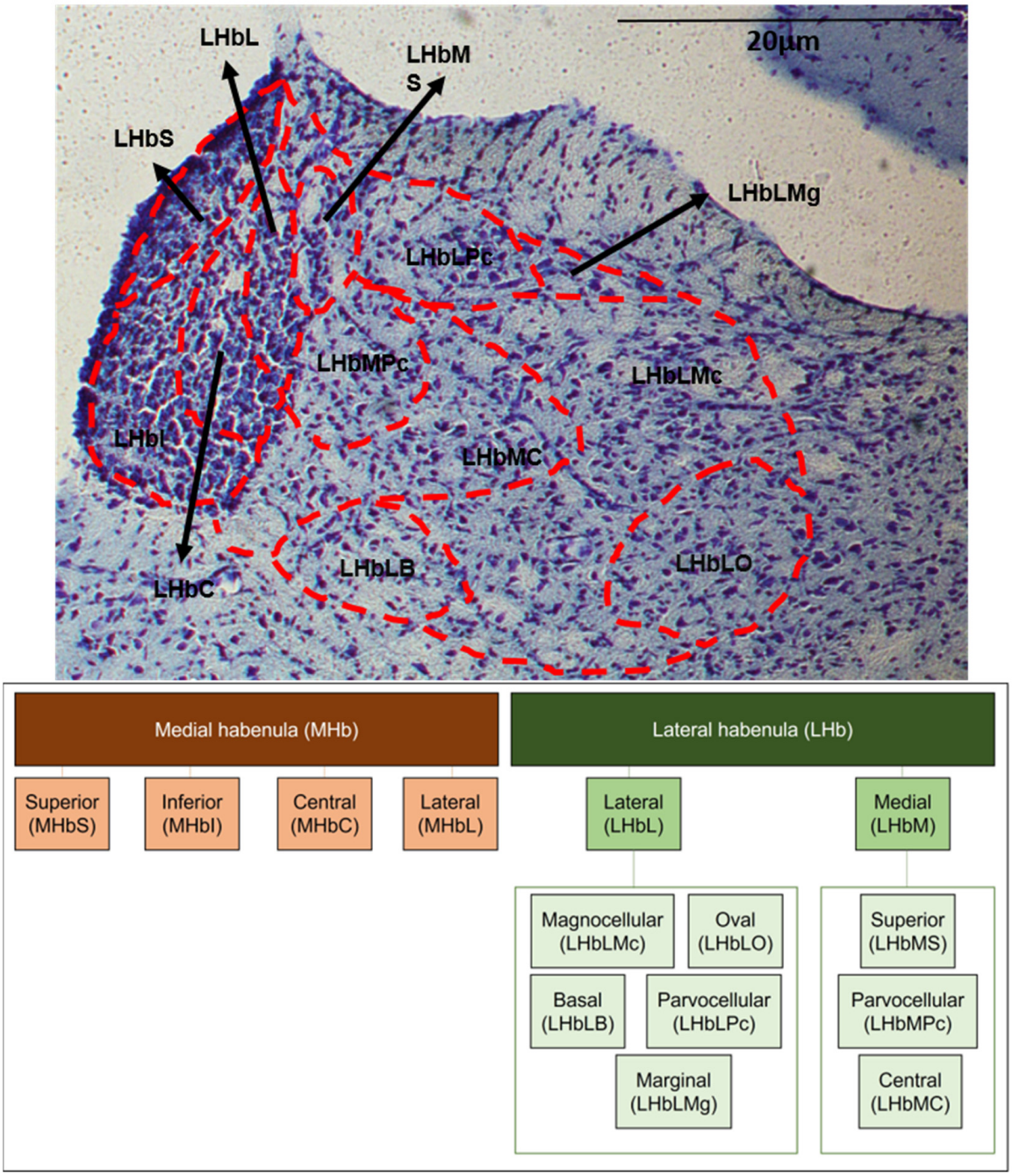

Figure 6. The subdivisions of the habenula in Nissl staining and schematic. Habenula was first divided into medial (MHb) and lateral (LHb) complexes. The medial complex (MHb) was divided into superior (MHbS), inferior (MHbI), central (MHbC) and lateral (MHbL) regions. The lateral complex (LHb) was subdivided into lateral (LHbL) and medial (LHbM) regions. The LHbL was further parcellated into magnocellular (LHbLMc), oval (LHbLO), basal (LHbLB), parvocellular (LHbLPc) and marginal (LHbLMg) parts, while the LHbM was parcellated into superior (LHbMS), parvocellular (LHbMPc) and central (LHbMC) parts.

4.8. Statistical Analyses

Data are presented as the mean ± standard error of the mean (SEM). The sample size calculation was performed as previously described [84]. Statistical analyses were conducted with GraphPad Prism 9.0 software (GraphPad Software Inc.; San Diego, CA, USA). The normal distribution of the samples was confirmed using the Shapiro–Wilk test. The results of the two-way shuttle boxes test were analyzed using two-way repeated measures analysis of variance (ANOVA) considering Factor 1 Group, Factor 2 Session, followed by Bonferroni post hoc test. The immunohistochemistry assay results were normalized by defining the control group as 100% and analyzed using one-way ANOVA followed by Tukey post hoc test. For all tests, $p < 0.05$ was considered statistically significant.

5. Conclusions

The data presented here suggest that specific subdivisions of the MHb and LHb have different activation patterns and astroglial immunoreactivity in animals presenting good and poor avoidance behavior. We hope that this detailed evaluation will provide the basis for further studies to better comprehend the individualized signature and connectivity of each habenular subdivision.

Author Contributions: G.F.A., A.C.P.C., D.d.O.M. and F.V.G. performed the experiments, analyzed the data and wrote the draft manuscript. M.J.R.J., R.L.P. and R.C.R.M. designed the study, analyzed the data and wrote the draft manuscript. All authors have read and agreed to the published version of the manuscript.

Funding: This research was supported by FAPESP grants to R.C.R.M. (#11/08575-7), A.C.P.C. (#18/18695-9) and F.V.G. (#13/20602-5), by Coordination for the Improvement of Higher Education Personnel (CAPES, GFA 88882.366209/2019-01).

Institutional Review Board Statement: All animal experiments were conducted and reported in accordance with the ARRIVE guidelines (http://www.nc3rs.org.uk/arrive-guidelines, accessed on 1 March 2022). The protocols used in this project were approved by the Ethics Committee on the Use of Animals at Hospital Sirio-Libanes (CEUA #2013/12); the date of approval is 8 January 2014, and it is valid to date.

Informed Consent Statement: Not applicable.

Data Availability Statement: The data generated and analyzed during the current study are available from the corresponding author upon reasonable request.

Acknowledgments: The authors are grateful to Bruno Gregnanin Pedron and all the staff of Hospital Sírio-Libanês.

Conflicts of Interest: The authors declare no commercial or financial relationships that could be construed as potential conflicts of interest.

References

1. Craske, M.G.; Stein, M.B.; Eley, T.C.; Milad, M.R.; Holmes, A.; Rapee, R.M.; Wittchen, H.-U. Anxiety Disorders. *Nat. Rev. Dis. Primer* **2017**, *3*, 17024. [CrossRef]
2. Wilmer, M.T.; Anderson, K.; Reynolds, M. Correlates of Quality of Life in Anxiety Disorders: Review of Recent Research. *Curr. Psychiatry Rep.* **2021**, *23*, 77. [CrossRef] [PubMed]
3. Moitra, E.; Herbert, J.D.; Forman, E.M. Behavioral Avoidance Mediates the Relationship between Anxiety and Depressive Symptoms among Social Anxiety Disorder Patients. *J. Anxiety Disord.* **2008**, *22*, 1205–1213. [CrossRef] [PubMed]
4. Bardeen, J.R.; Tull, M.T.; Stevens, E.N.; Gratz, K.L. Exploring the Relationship between Positive and Negative Emotional Avoidance and Anxiety Symptom Severity: The Moderating Role of Attentional Control. *J. Behav. Ther. Exp. Psychiatry* **2014**, *45*, 415–420. [CrossRef] [PubMed]
5. LeDoux, J.E. *Anxious: Using the Brain to Understand and Treat Fear and Anxiety*; Viking: New York, NY, USA, 2015; ISBN 978-0-670-01533-7.
6. Campese, V.D.; Sears, R.M.; Moscarello, J.M.; Diaz-Mataix, L.; Cain, C.K.; LeDoux, J.E. The Neural Foundations of Reaction and Action in Aversive Motivation. *Curr. Top. Behav. Neurosci.* **2016**, *27*, 171–195. [CrossRef] [PubMed]

7. Martinez, R.C.R.; Gupta, N.; Lázaro-Muñoz, G.; Sears, R.M.; Kim, S.; Moscarello, J.M.; LeDoux, J.E.; Cain, C.K. Active vs. Reactive Threat Responding Is Associated with Differential c-Fos Expression in Specific Regions of Amygdala and Prefrontal Cortex. *Learn. Mem.* **2013**, *20*, 446–452. [CrossRef] [PubMed]
8. Adamec, R.; Young, B. Neuroplasticity in Specific Limbic System Circuits May Mediate Specific Kindling Induced Changes in Animal Affect—Implications for Understanding Anxiety Associated with Epilepsy. *Neurosci. Biobehav. Rev.* **2000**, *24*, 705–723. [CrossRef]
9. Baker, P.M.; Mathis, V.; Lecourtier, L.; Simmons, S.C.; Nugent, F.S.; Hill, S.; Mizumori, S.J.Y. Lateral Habenula Beyond Avoidance: Roles in Stress, Memory, and Decision-Making With Implications for Psychiatric Disorders. *Front. Syst. Neurosci.* **2022**, *16*, 826475. [CrossRef]
10. Li, B.; Piriz, J.; Mirrione, M.; Chung, C.; Proulx, C.D.; Schulz, D.; Henn, F.; Malinow, R. Synaptic Potentiation onto Habenula Neurons in Learned Helplessness Model of Depression. *Nature* **2011**, *470*, 535–539. [CrossRef]
11. Antunes, G.; Pinheiro Campos, A.C.; Assis, D.; Venetucci Gouveia, F.; Seno, M.; Pagano, R.; Martinez, R. Habenula Activation Patterns in a Preclinical Model of Neuropathic Pain Accompanied by Depressive-like Behaviour. *PLoS ONE* **2022**, *17*, e0271295. [CrossRef]
12. Meye, F.J.; Lecca, S.; Valentinova, K.; Mameli, M. Synaptic and Cellular Profile of Neurons in the Lateral Habenula. *Front. Hum. Neurosci.* **2013**, *7*, 860. [CrossRef] [PubMed]
13. Wang, D.; Li, Y.; Feng, Q.; Guo, Q.; Zhou, J.; Luo, M. Learning Shapes the Aversion and Reward Responses of Lateral Habenula Neurons. *eLife* **2017**, *6*, e23045. [CrossRef] [PubMed]
14. Herkenham, M.; Nauta, W.J. Efferent Connections of the Habenular Nuclei in the Rat. *J. Comp. Neurol.* **1979**, *187*, 19–47. [CrossRef] [PubMed]
15. Gouveia, F.V.; Ibrahim, G.M. Habenula as a Neural Substrate for Aggressive Behavior. *Front. Psychiatry* **2022**, *13*, 817302. [CrossRef]
16. Hikosaka, O. The Habenula: From Stress Evasion to Value-Based Decision-Making. *Nat. Rev. Neurosci.* **2010**, *11*, 503–513. [CrossRef]
17. Bianco, I.H.; Wilson, S.W. The Habenular Nuclei: A Conserved Asymmetric Relay Station in the Vertebrate Brain. *Philos. Trans. R. Soc. B Biol. Sci.* **2009**, *364*, 1005–1020. [CrossRef]
18. Boulos, L.-J.; Darcq, E.; Kieffer, B.L. Translating the Habenula—From Rodents to Humans. *Biol. Psychiatry* **2017**, *81*, 296–305. [CrossRef]
19. Bromberg-Martin, E.S.; Matsumoto, M.; Hikosaka, O. Distinct Tonic and Phasic Anticipatory Activity in Lateral Habenula and Dopamine Neurons. *Neuron* **2010**, *67*, 144–155. [CrossRef] [PubMed]
20. Metzger, M.; Souza, R.; Lima, L.B.; Bueno, D.; Gonçalves, L.; Sego, C.; Donato, J., Jr.; Shammah-Lagnado, S.J. Habenular Connections with the Dopaminergic and Serotonergic System and Their Role in Stress-Related Psychiatric Disorders. *Eur. J. Neurosci.* **2021**, *53*, 65–88. [CrossRef] [PubMed]
21. Lawther, A.J.; Hale, M.W.; Lowry, C.A. Chapter 29—Serotonin and the Neurobiology of Anxious States. In *Handbook of Behavioral Neuroscience*; Müller, C.P., Cunningham, K.A., Eds.; Handbook of the Behavioral Neurobiology of Serotonin; Elsevier: Amsterdam, The Netherlands, 2020; Volume 31, pp. 505–520.
22. Song, M.; Jo, Y.S.; Lee, Y.-K.; Choi, J.-S. Lesions of the Lateral Habenula Facilitate Active Avoidance Learning and Threat Extinction. *Behav. Brain Res.* **2017**, *318*, 12–17. [CrossRef]
23. Shumake, J.; Ilango, A.; Scheich, H.; Wetzel, W.; Ohl, F.W. Differential Neuromodulation of Acquisition and Retrieval of Avoidance Learning by the Lateral Habenula and Ventral Tegmental Area. *J. Neurosci.* **2010**, *30*, 5876–5883. [CrossRef] [PubMed]
24. Ransom, B.R.; Ransom, C.B. Astrocytes: Multitalented Stars of the Central Nervous System. *Methods Mol. Biol. Clifton NJ* **2012**, *814*, 3–7. [CrossRef]
25. Wang, Y.; Qu, P.; Sun, Y.; Li, Z.; Liu, L.; Yang, L. Association between Increased Inflammatory Cytokine Expression in the Lateral Habenular Nucleus and Depressive-like Behavior Induced by Unpredictable Chronic Stress in Rats. *Exp. Neurol.* **2022**, *349*, 113964. [CrossRef] [PubMed]
26. Felger, J.C. Imaging the Role of Inflammation in Mood and Anxiety-Related Disorders. *Curr. Neuropharmacol.* **2018**, *16*, 533–558. [CrossRef] [PubMed]
27. Pekny, M.; Wilhelmsson, U.; Pekna, M. The Dual Role of Astrocyte Activation and Reactive Gliosis. *Neurosci. Lett.* **2014**, *565*, 30–38. [CrossRef] [PubMed]
28. Nielson, H.C.; McIver, A.H. Cold Stress and Habenular Lesion Effects on Rat Behaviors. *J. Appl. Physiol.* **1966**, *21*, 655–660. [CrossRef]
29. Macdougall, J.M.; Van Hoesen, G.W.; Mitchell, J.C. Anatomical Organization of Septal Projections in Maintenance of DRL Behavior in Rats. *J. Comp. Physiol. Psychol.* **1969**, *68*, 568–575. [CrossRef]
30. Tigner, J.C. Impairment of One-Way Active Avoidance in Rats with Habenular or Dorsomedial Thalamic Lesions. *Psychon. Sci.* **1972**, *27*, 7–8. [CrossRef]
31. Andres, K.H.; Düring, M.V.; Veh, R.W. Subnuclear Organization of the Rat Habenular Complexes. *J. Comp. Neurol.* **1999**, *407*, 130–150. [CrossRef]
32. Namboodiri, V.M.K.; Rodriguez-Romaguera, J.; Stuber, G.D. The Habenula. *Curr. Biol.* **2016**, *26*, R873–R877. [CrossRef]

33. Yamaguchi, T.; Danjo, T.; Pastan, I.; Hikida, T.; Nakanishi, S. Distinct Roles of Segregated Transmission of the Septo-Habenular Pathway in Anxiety and Fear. *Neuron* **2013**, *78*, 537–544. [CrossRef] [PubMed]
34. Ren, J.; Qin, C.; Hu, F.; Tan, J.; Qiu, L.; Zhao, S.; Feng, G.; Luo, M. Habenula "Cholinergic" Neurons Co-Release Glutamate and Acetylcholine and Activate Postsynaptic Neurons via Distinct Transmission Modes. *Neuron* **2011**, *69*, 445–452. [CrossRef]
35. Hsu, Y.-W.A.; Tempest, L.; Quina, L.A.; Wei, A.D.; Zeng, H.; Turner, E.E. Medial Habenula Output Circuit Mediated by A5 Nicotinic Receptor-Expressing GABAergic Neurons in the Interpeduncular Nucleus. *J. Neurosci.* **2013**, *33*, 18022. [CrossRef] [PubMed]
36. Morley, B.J. The Interpeduncular Nucleus. *Int. Rev. Neurobiol.* **1986**, *28*, 157–182. [CrossRef] [PubMed]
37. Fowler, C.D.; Tuesta, L.; Kenny, P.J. Role of A5* Nicotinic Acetylcholine Receptors in the Effects of Acute and Chronic Nicotine Treatment on Brain Reward Function in Mice. *Psychopharmacology* **2013**. [CrossRef]
38. Lawson, R.P.; Seymour, B.; Loh, E.; Lutti, A.; Dolan, R.J.; Dayan, P.; Weiskopf, N.; Roiser, J.P. The Habenula Encodes Negative Motivational Value Associated with Primary Punishment in Humans. *Proc. Natl. Acad. Sci. USA* **2014**, *111*, 11858–11863. [CrossRef]
39. Klemm, W.R. Habenular and Interpeduncularis Nuclei: Shared Components in Multiple-Function Networks. *Med. Sci. Monit. Int. Med. J. Exp. Clin. Res.* **2004**, *10*, RA261–RA273.
40. Aizawa, H.; Kobayashi, M.; Tanaka, S.; Fukai, T.; Okamoto, H. Molecular Characterization of the Subnuclei in Rat Habenula. *J. Comp. Neurol.* **2012**, *520*, 4051–4066. [CrossRef]
41. Staines, W.A.; Yamamoto, T.; Dewar, K.M.; Daddona, P.E.; Geiger, J.D.; Nagy, J.I. Distribution, Morphology and Habenular Projections of Adenosine Deaminase-Containing Neurons in the Septal Area of Rat. *Brain Res.* **1988**, *455*, 72–87. [CrossRef]
42. Hillman, D.; Chen, S.; Aung, T.T.; Cherksey, B.; Sugimori, M.; Llinás, R.R. Localization of P-Type Calcium Channels in the Central Nervous System. *Proc. Natl. Acad. Sci. USA* **1991**, *88*, 7076–7080. [CrossRef]
43. Ding, Y.Q.; Kaneko, T.; Nomura, S.; Mizuno, N. Immunohistochemical Localization of Mu-Opioid Receptors in the Central Nervous System of the Rat. *J. Comp. Neurol.* **1996**, *367*, 375–402. [CrossRef]
44. Kawaja, M.D.; Flumerfelt, B.A.; Hrycyshyn, A.W. Topographical and Ultrastructural Investigation of the Habenulo-Interpeduncular Pathway in the Rat: A Wheat Germ Agglutinin-Horseradish Peroxidase Anterograde Study. *J. Comp. Neurol.* **1988**, *275*, 117–127. [CrossRef]
45. Okamoto, H.; Agetsuma, M.; Aizawa, H. Genetic Dissection of the Zebrafish Habenula, a Possible Switching Board for Selection of Behavioral Strategy to Cope with Fear and Anxiety. *Dev. Neurobiol.* **2012**, *72*, 386–394. [CrossRef] [PubMed]
46. Hsu, Y.-W.A.; Morton, G.; Guy, E.G.; Wang, S.D.; Turner, E.E. Dorsal Medial Habenula Regulation of Mood-Related Behaviors and Primary Reinforcement by Tachykinin-Expressing Habenula Neurons. *eNeuro* **2016**, *3*, ENEURO.0109-16.2016. [CrossRef] [PubMed]
47. Melani, R.; Von Itter, R.; Jing, D.; Koppensteiner, P.; Ninan, I. Opposing Effects of an Atypical Glycinergic and Substance P Transmission on Interpeduncular Nucleus Plasticity. *Neuropsychopharmacol. Off. Publ. Am. Coll. Neuropsychopharmacol.* **2019**, *44*, 1828–1836. [CrossRef]
48. Lee, S.; Jha, M.K.; Suk, K. Lipocalin-2 in the Inflammatory Activation of Brain Astrocytes. *Crit. Rev. Immunol.* **2015**, *35*, 77–84. [CrossRef]
49. Lushnikova, I.; Skibo, G.; Muller, D.; Nikonenko, I. Synaptic Potentiation Induces Increased Glial Coverage of Excitatory Synapses in CA1 Hippocampus. *Hippocampus* **2009**, *19*, 753–762. [CrossRef]
50. Wirtshafter, D. The Role of Interpeduncular Connections with the Tegmentum in Avoidance Learning. *Physiol. Behav.* **1981**, *26*, 985–989. [CrossRef]
51. Durieux, L.; Herbeaux, K.; Borcuk, C.; Hildenbrand, C.; Andry, V.; Goumon, Y.; Barbelivien, A.; Mathis, C.; Bataglia, D.; Majchrzak, M.; et al. Functional Brain-Wide Network Mapping during Acute Stress Exposure in Rats: Interaction between the Lateral Habenula and Cortical, Amygdalar, Hypothalamic and Monoaminergic Regions. *Eur. J. Neurosci.* **2022**, *56*, 5154–5176. [CrossRef]
52. Kovács, L.Á.; Füredi, N.; Ujvári, B.; Golgol, A.; Gaszner, B. Age-Dependent FOSB/ΔFOSB Response to Acute and Chronic Stress in the Extended Amygdala, Hypothalamic Paraventricular, Habenular, Centrally-Projecting Edinger-Westphal, and Dorsal Raphe Nuclei in Male Rats. *Front. Aging Neurosci.* **2022**, *14*, 862098. [CrossRef]
53. Febbraro, F.; Svenningsen, K.; Tran, T.P.; Wiborg, O. Neuronal Substrates Underlying Stress Resilience and Susceptibility in Rats. *PLoS ONE* **2017**, *12*, e0179434. [CrossRef] [PubMed]
54. Dolzani, S.D.; Baratta, M.V.; Amat, J.; Agster, K.L.; Saddoris, M.P.; Watkins, L.R.; Maier, S.F. Activation of a Habenulo-Raphe Circuit Is Critical for the Behavioral and Neurochemical Consequences of Uncontrollable Stress in the Male Rat. *eNeuro* **2016**, *3*, ENEURO.0229-16.2016. [CrossRef] [PubMed]
55. Cobb, J.A.; O'Neill, K.; Milner, J.; Mahajan, G.J.; Lawrence, T.J.; May, W.L.; Miguel-Hidalgo, J.; Rajkowska, G.; Stockmeier, C.A. Density of GFAP-Immunoreactive Astrocytes Is Decreased in Left Hippocampi in Major Depressive Disorder. *Neuroscience* **2016**, *316*, 209–220. [CrossRef]
56. Gosselin, R.-D.; Gibney, S.; O'Malley, D.; Dinan, T.G.; Cryan, J.F. Region Specific Decrease in Glial Fibrillary Acidic Protein Immunoreactivity in the Brain of a Rat Model of Depression. *Neuroscience* **2009**, *159*, 915–925. [CrossRef]
57. Isaacson, R.L.; Fahey, J.M.; Mughairbi, F.A. Environmental Conditions Unexpectedly Affect the Long-Term Extent of Cell Death Following an Hypoxic Episode. *Ann. N. Y. Acad. Sci.* **2003**, *993*, 179–194; discussion 195–196. [CrossRef] [PubMed]

58. Featherstone, R.E.; Fleming, A.S.; Ivy, G.O. Plasticity in the Maternal Circuit: Effects of Experience and Partum Condition on Brain Astrocyte Number in Female Rats. *Behav. Neurosci.* **2000**, *114*, 158–172. [CrossRef] [PubMed]
59. Katz, R.J.; Roth, K.A.; Carroll, B.J. Acute and Chronic Stress Effects on Open Field Activity in the Rat: Implications for a Model of Depression. *Neurosci. Biobehav. Rev.* **1981**, *5*, 247–251. [CrossRef]
60. Dafny, N.; Qiao, J.T. Habenular Neuron Responses to Noxious Input Are Modified by Dorsal Raphe Stimulation. *Neurol. Res.* **1990**, *12*, 117–121. [CrossRef]
61. Haun, F.; Eckenrode, T.; Murray, M. Habenula and Thalamus Cell Transplants Restore Normal Sleep Behaviors Disrupted by Denervation of the Interpeduncular Nucleus. *J. Neurosci.* **1992**, *12*, 3282–3290. [CrossRef]
62. Sutherland, R.J. The Dorsal Diencephalic Conduction System: A Review of the Anatomy and Functions of the Habenular Complex. *Neurosci. Biobehav. Rev.* **1982**, *6*, 1–13. [CrossRef]
63. Bradbury, M.J.; Cascio, C.S.; Scribner, K.A.; Dallman, M.F. Stress-Induced Adrenocorticotropin Secretion: Diurnal Responses and Decreases during Stress in the Evening Are Not Dependent on Corticosterone. *Endocrinology* **1991**, *128*, 680–688. [CrossRef]
64. Rusak, B. Vertebrate Behavioral Rhythms. In *Biological Rhythms*; Aschoff, J., Ed.; Springer: Boston, MA, USA, 1981; pp. 183–213; ISBN 978-1-4615-6552-9.
65. Chastrette, N.; Pfaff, D.W.; Gibbs, R.B. Effects of Daytime and Nighttime Stress on Fos-like Immunoreactivity in the Paraventricular Nucleus of the Hypothalamus, the Habenula, and the Posterior Paraventricular Nucleus of the Thalamus. *Brain Res.* **1991**, *563*, 339–344. [CrossRef] [PubMed]
66. Juárez-Leal, I.; Carretero-Rodríguez, E.; Almagro-García, F.; Martínez, S.; Echevarría, D.; Puelles, E. Stria Medullaris Innervation Follows the Transcriptomic Division of the Habenula. *Sci. Rep.* **2022**, *12*, 10118. [CrossRef]
67. Tsuneoka, Y.; Funato, H. Cellular Composition of the Preoptic Area Regulating Sleep, Parental, and Sexual Behavior. *Front. Neurosci.* **2021**, *15*, 649159. [CrossRef] [PubMed]
68. Beckstead, R.M.; Domesick, V.B.; Nauta, W.J. Efferent Connections of the Substantia Nigra and Ventral Tegmental Area in the Rat. *Brain Res.* **1979**, *175*, 191–217. [CrossRef] [PubMed]
69. Parent, A.; Gravel, S.; Boucher, R. The Origin of Forebrain Afferents to the Habenula in Rat, Cat and Monkey. *Brain Res. Bull.* **1981**, *6*, 23–38. [CrossRef]
70. Greatrex, R.M.; Phillipson, O.T. Demonstration of Synaptic Input from Prefrontal Cortex to the Habenula in the Rat. *Brain Res.* **1982**, *238*, 192–197. [CrossRef]
71. Liguz-Lecznar, M.; Dobrzanski, G.; Kossut, M. Somatostatin and Somatostatin-Containing Interneurons-From Plasticity to Pathology. *Biomolecules* **2022**, *12*, 312. [CrossRef]
72. Li, H.; Eid, M.; Pullmann, D.; Chao, Y.S.; Thomas, A.A.; Jhou, T.C. Entopeduncular Nucleus Projections to the Lateral Habenula Contribute to Cocaine Avoidance. *J. Neurosci. Off. J. Soc. Neurosci.* **2021**, *41*, 298–306. [CrossRef]
73. Corkrum, M.; Araque, A. Astrocyte-Neuron Signaling in the Mesolimbic Dopamine System: The Hidden Stars of Dopamine Signaling. *Neuropsychopharmacology* **2021**, *46*, 1864–1872. [CrossRef]
74. Antunes, G.F.; Gouveia, F.V.; Rezende, F.S.; de Jesus Seno, M.D.; de Carvalho, M.C.; de Oliveira, C.C.; Dos Santos, L.C.T.; de Castro, M.C.; Kuroki, M.A.; Teixeira, M.J.; et al. Dopamine Modulates Individual Differences in Avoidance Behavior: A Pharmacological, Immunohistochemical, Neurochemical and Volumetric Investigation. *Neurobiol. Stress* **2020**, *12*, 100219. [CrossRef] [PubMed]
75. de Oliveira, C.C.; Gouveia, F.V.; de Castro, M.C.; Kuroki, M.A.; dos Santos, L.C.T.; Fonoff, E.T.; Teixeira, M.J.; Otoch, J.P.; Martinez, R.C.R. A Window on the Study of Aversive Instrumental Learning: Strains, Performance, Neuroendocrine, and Immunologic Systems. *Front. Behav. Neurosci.* **2016**, *10*. [CrossRef] [PubMed]
76. Lázaro-Muñoz, G.; LeDoux, J.E.; Cain, C.K. Sidman Instrumental Avoidance Initially Depends on Lateral and Basal Amygdala and Is Constrained by Central Amygdala-Mediated Pavlovian Processes. *Biol. Psychiatry* **2010**, *67*, 1120–1127. [CrossRef]
77. Blanchard, D.C.; Blanchard, R.J. Ethoexperimental Approaches to the Biology of Emotion. *Annu. Rev. Psychol.* **1988**, *39*, 43–68. [CrossRef] [PubMed]
78. Deutsch, E.W.; Ball, C.A.; Berman, J.J.; Bova, G.S.; Brazma, A.; Bumgarner, R.E.; Campbell, D.; Causton, H.C.; Christiansen, J.H.; Daian, F.; et al. Minimum Information Specification for in Situ Hybridization and Immunohistochemistry Experiments (MISFISHIE). *Nat. Biotechnol.* **2008**, *26*, 305–312. [CrossRef] [PubMed]
79. Howat, W.J.; Lewis, A.; Jones, P.; Kampf, C.; Pontén, F.; van der Loos, C.M.; Gray, N.; Womack, C.; Warford, A. Antibody Validation of Immunohistochemistry for Biomarker Discovery: Recommendations of a Consortium of Academic and Pharmaceutical Based Histopathology Researchers. *Methods* **2014**, *70*, 34–38. [CrossRef]
80. Martinez, R.C.; Carvalho-Netto, E.F.; Ribeiro-Barbosa, E.R.; Baldo, M.V.C.; Canteras, N.S. Amygdalar Roles during Exposure to a Live Predator and to a Predator-Associated Context. *Neuroscience* **2011**, *172*, 314–328. [CrossRef]
81. Martinez, R.C.R.; Carvalho-Netto, E.F.; Amaral, V.C.S.; Nunes-de-Souza, R.L.; Canteras, N.S. Investigation of the Hypothalamic Defensive System in the Mouse. *Behav. Brain Res.* **2008**, *192*, 185–190. [CrossRef]
82. Seno, M.D.J.; Assis, D.V.; Gouveia, F.; Antunes, G.F.; Kuroki, M.; Oliveira, C.C.; Santos, L.C.T.; Pagano, R.L.; Martinez, R.C.R. The Critical Role of Amygdala Subnuclei in Nociceptive and Depressive-like Behaviors in Peripheral Neuropathy. *Sci. Rep.* **2018**, *8*, 13608. [CrossRef]

83. Paxinos, G.; Watson, C. *The Rat Brain in Stereotaxic Coordinates*; Elsevier Science: Amsterdam, The Netherlands, 2013; ISBN 978-0-12-391949-6.
84. Charan, J.; Kantharia, N.D. How to Calculate Sample Size in Animal Studies? *J. Pharmacol. Pharmacother.* **2013**, *4*, 303–306. [CrossRef]